ORIGINAL RESEARCH

AS-605240 Blunts Osteoporosis by Inhibition of Bone Resorption

Jiacheng Sun[1,2,*], Guoping Cai[1,2,*], Jinlong Shen [1,2], Pu Cheng [1,2], Jiapeng Zhang [1,2], Dengteng Jiang[1,2], Xianquan Xu[1,2], Fangying Lu[1,2], Lihua Chen [1,2], Haixiao Chen[1,2]

[1]Department of Orthopaedics, Taizhou Hospital Affiliated to Wenzhou Medical University, Linhai, Zhejiang Province, People's Republic of China; [2]Bone Development and Metabolism Research Center of Taizhou Hospital, Linhai, Zhejiang Province, People's Republic of China

*These authors contributed equally to this work

Correspondence: Haixiao Chen; Lihua Chen, Department of Orthopaedics, Taizhou Hospital Affiliated to Wenzhou Medical University, N.150 Ximen Road of Linhai City, Taizhou, Zhejiang Province, People's Republic of China, Tel +86 15268400288, +86 13757624851, Email sun846231221@163.com; lhchen2008@126.com

Background: Osteoporosis is a metabolic bone disease. Osteoclasts are significantly involved in the pathogenesis of osteoporosis. AS-605240 (AS) is a small molecule PI3K-γ inhibitor and is less toxic compared to pan-PI3K inhibitors. AS also exerts multiple biological effects including anti-inflammatory, anti-tumor, and myocardial remodeling promotion. However, the involvement of AS in the differentiation and functions of osteoclasts and the effect of AS in treating patients with osteoporosis is still unclear.

Purpose: This study aimed to investigate if AS inhibits the differentiation of osteoclasts and resorption of the bones induced by M-CSF and RANKL. Next, we evaluated the therapeutic effects of AS on bone loss in ovariectomy (OVX)-induced osteoporosis mice models.

Methods: We stimulated bone marrow-derived macrophages with an osteoclast differentiation medium containing different AS concentrations for 6 days or 5μM AS at different times. Next, we performed tartrate-resistant acid phosphatase (TRAP) staining, bone resorption assay, F-actin ring fluorescence, real-time quantitative polymerase chain reaction (RT-qPCR), and Western blotting (WB). Next, MC3T3-E1s (pre-osteoblast cells) were differentiated to osteoblast by stimulating the cells with varying AS concentrations. Next, we performed alkaline phosphatase (ALP) staining, RT-qPCR, and WB on these cells. We established an OVX-induced osteoporosis mice model and treated the mice with 20mg/kg of AS. Finally, we extracted the femurs and performed micro-CT scanning, H&E, and TRAP staining.

Results: AS inhibits the formation of osteoclasts and resorption of bone triggered by RANKL by inhibiting the PI3K/Akt signaling pathway. Furthermore, AS enhances the differentiation of osteoblasts and inhibits bone loss due to OVX in vivo.

Conclusion: AS inhibits osteoclast production and enhances osteoblast differentiation in mice, thus providing a new therapeutic approach for treating patients with osteoporosis.

Keywords: AS-605240, PI3Kγ, osteoclast, PI3K/Akt, osteoporosis

Introduction

Bone growth is a dynamic process and involves continuous remodeling.[1] It primarily depends on the homeostasis between the resorption of osteoclasts and the formation of osteoblasts.[2,3] Alterations in the homeostasis between the resorption and formation of bones occur in several skeletal diseases, such as osteoporosis and osteopetrosis.[4] The primary cause of such skeletal diseases is aberrant osteoclast activity; hence osteoclast activity could be an important therapeutic target.[5,6]

Osteoclasts become multinucleated when monocytes/macrophage progenitor cells fuse.[7] In vitro formation and differentiation of osteoclasts are primarily mediated by macrophage colony-stimulating factor (M-CSF) and receptor activator nuclear factor-kappa B ligand (RANKL).[8,9] The binding of M-CSF binds to its receptor, c-Fms, promotes the survival as well as the proliferation of osteoclast precursors.[10] The phosphatidylinositol 3-kinase/protein kinase B (PI3K/

1275

Akt), nuclear factor-κB (NF-κB), and mitogen-activated protein kinase (MAPK) signaling pathways are associated with the interaction between RANKL and its receptor RANK.[11–13] Furthermore, these signaling pathways induce the transcription of the downstream molecules NFATc1 and c-Fos. Several osteoclast-related genes, such as acid phosphatase 5 (ACP5), cathepsin K (CTSK), and dendritic cell-specific transmembrane protein (DC-STAMP), are activated by transcription factor NFATc1.[14,15] Therefore, inhibiting signal pathways mediated by RANKL during osteoclast formation could serve as a therapeutic strategy for treating patients with osteolytic diseases associated with osteoclasts, such as osteoporosis.[16]

AS-605240 (AS) is a small molecule PI3K-γ inhibitor. They primarily act on the hematopoietic system and are less toxic than pan-PI3K inhibitor.[17] Previous studies have shown that AS exerts anti-inflammatory effects in rheumatoid arthritis, glomerulonephritis, chronic obstructive pulmonary disease, and other inflammatory diseases and anticancer effects in breast cancers. Moreover, AS promotes cardiac remodeling after myocardial infarction.[18–21] PI3K/AKT inhibitors, such as Alpinetin, AZD1390, etc., have been reported to alleviate osteoclast-associated bone metabolic disorders by inhibiting osteoclast differentiation.[22,23] However, the effect of AS on osteoclast-related bone loss is unclear. Therefore, this study aimed to determine the influence of AS on the differentiation and functions of osteoclasts in the presence of RANKL. Our results revealed that AS inhibits osteoclast generation and reduces the bone reabsorption ability of osteoclasts. Additionally, AS attenuated NFATc1-induced osteoclasts via the mechanism of inhibiting the PI3K/ Akt signaling pathways. Furthermore, interfering with the osteoblast differentiation of MC3T3-E1 cells revealed that AS promotes osteoblast differentiation. Finally, in vivo studies suggested that AS could protect against bone loss in the ovariectomy (OVX)-induced osteoporosis mice models. Therefore, our results indicate that AS could be used as a therapeutic strategy for treating osteoclast-related osteolytic diseases, such as osteoporosis.

Materials and Methods
Media and Reagents
AS-605240 (purity>99%) was obtained from MCE (Shanghai, China). Alpha-minimum essential medium (αMEM), trypsin-ethylene diamine tetraacetic acid (EDTA) solution, and penicillin/streptomycin (P/S) solution were purchased from Bio-Channel (Nanjing, China). We procured fetal bovine serum (FBS) from Avantor (Molendinar, Australia). Cell counting kit-8 (CCK-8) was supplied by MCE (Shanghai, China). We purchased mouse recombinant M-CSF and RANKL from R&D Systems (Minneapolis, USA). We purchased primary antibodies against the total and phosphorylated proteins, including β-actin (#4970, 1:1000), PI3K (#4295, 1:1000), p-PI3K (#17366, 1:1000), Akt (#4691, 1:1000), p-Akt (#4060, 1:1000), P65 (#8242, 1:1000), p-P65 (#3033, 1:1000), IκBα (#4814, 1:1000), p-IκBα (#2859, 1:1000), P38 (#8690, 1:1000), p-P38 (#4511S, 1:1000), ERK (#4695, 1:1000), p-ERK (#4370, 1:1000), JNK (#9252, 1:1000), p-JNK (#9255, 1:1000) and RUNX2 (#12556, 1:1000) from Cell Signaling Technology (Danvers, USA). We obtained c-Fos (ab222699, 1:1000) and NFATc1 (ab2722, 1:1000) from Abcam (Shanghai, China), and the dilution of the primary antibodies was obtained from Beyotime Biotechnology (Shanghai, China). We purchased a secondary antibody (#S0001, 1:20000) from Affbiotech (Changzhou, China).

Cell Culture
Primary bone marrow macrophages (BMMs) were extracted from the tibia and femur of C57BL/6 male mice (6 weeks old). First, the femur and tibia were separated using sterile scissors, and the bone marrow was flushed using a 1 mL syringe. Next, we seeded the cells into 100 mm cell culture dishes and cultured them in αMEM supplemented with 1% P/ S, 30ng/mL M-CSF, and 10% FBS. MC3T3-E1s (pre-osteoblast cells) were cultured in α-MEM containing 1% P/S and 10% FBS and maintained in an incubator at 37°C and 5% CO_2. The cells were cultured until 90% confluency.

Cytotoxicity Assay
BMMs were seeded into 96-well plates at an initial density of 8000 cells per well, while MC3T3-E1s were inoculated at a density of 5000 cells per well. To evaluate the cytotoxicity, on the next day, we treated the cells with 0, 0.039, 0.078, 0.156, 0.313, 0.625, 1.25, 2.5, 5, and 10μM of AS for 24, 48, 72, and 96 hours. Next, the cells were treated with CCK-8

regent for 2 hours. Finally, the absorbance was measured using the Multiskan FC microplate photometer (Thermo Fisher Scientific, MA, USA).

Osteoclast Differentiation Assay in vitro

After growing to the appropriate confluence on 100mm cell culture dishes, BMMs were digested by pancreatic enzymes and inoculated in 96-well plates at the same density as described above. On the following day, the medium in the 96-well plate was replaced with osteoclast differentiation medium containing 50ng/mL RANKL, 30ng/mL M-CSF, and increasing concentrations of AS (0, 1.25, 2.5, 5μM) and changed every other day. On day 6, we washed the cells with phosphate-buffered saline (PBS) thrice and fixed them using 4% paraformaldehyde (PFA) for 40 minutes. Finally, cells were stained with tartrate-resistant acid phosphatase (TRAP) reagent, and TRAP+ cells with > three nuclei were identified as osteoclasts.

Bone Absorption Assay in vitro

First, 8000 BMMs/well were seeded onto the bone fragments of bovines. Next, cells were treated with osteoclast differentiation medium, and 0, 1.25, 2.5, and 5.0μM of AS till mature osteoclasts were observed. Subsequently, we removed adhered cells from the bone fragments of bovine. We employed scanning electron microscopy to capture the resorption pit images, and the bone resorption area was quantified using "Image J."

Immunofluorescence for F-Actin Ring

For osteoclast differentiation, cells were treated with or without varying AS concentrations for 6 days. Next, cells were fixed with 4% PFA for 40 minutes and permeabilized with 0.1% Triton X-100 for 10 minutes, respectively. Next, the cells were stained with YF 488-Phalloidin (Bioscience, Shanghai, China) in the darkness for 20 minutes at room temperature (RT). Next, the cells were washed with PBS thrice and counterstained with an antifade mounting medium containing DAPI (Beyotime, Beijing, China) for 10 minutes. Finally, an immunofluorescence microscope was utilized for observing F-actin rings.

In vitro Osteoblast Differentiation Assay

MC3T3-E1s were grown until confluent, digested using pancreatic enzymes, and $5×10^4$ cells/well were seeded in 12-well plates. Next, we replaced the medium with osteogenic differentiation medium (αMEM + 10mM β-glycerophosphate + 50μM ascorbic acid + 100nM dexamethasone) and 0, 0.31, 0.63, and 1.25μM of AS every alternate day for 7 days. Next, cells were washed with PBS thrice and fixed with 4% PFA for 30 minutes. Finally, cells were stained using an alkaline phosphatase (ALP) reagent.

RNA Extraction and Real-Time Quantitative Polymerase Chain Reaction (RT-qPCR)

We seeded $2×10^5$ BMMs/well in a 6-well plate. The culture medium and replaced with fresh osteoclast differentiation medium + 0, 1.25, 2.5, and 5μM of AS. The cells were cultured for 5 days. Next, MC3T3-E1s were treated with 0, 0.31, 0.62, and 1.25μM of AS for 5 days for osteogenic differentiation. On day 5, we extracted total RNA using RNAiso Plus (Takara, Otsu, Japan). RNA was reverse transcribed into cDNA using the HiFiScript cDNA Synthesis Kit (Cwbio, Beijing, China). Finally, RT-qPCR was performed using the ChamQ Universal SYBR qPCR Master Mix (Vazyme, Nanjing, China) on an Applied Biosystems 7300 PCR System (Thermo Fisher Scientific) in triplicates based on the protocols specified by manufacturers. Table 1 shows primer sequences. In addition, GAPDH served as a housekeeping gene.

Western Blotting (WB)

We inoculated BMMs at a density of $2×10^5$ cells/well in 6-well plates and cultured using osteoclast differentiation medium with or without 5μM of AS for 0, 1, 3, and 5 days to analyze the effect of AS on c-Fos and NFATc1. Moreover, for inducing osteoclast differentiation, we inoculated $2×10^5$ BMMs/well in 6-well plates and cultured using osteoclast differentiation medium + 0, 1.25, 2.5, and 5μM of AS for 5 days. To determine the effect of AS on the NF-κB, MAPKs,

Table 1 Primers Sequences for Real-Time PCR

Gene		Primer sequences (5′ → 3′)
Acp5	Forward	CACTCCCACCCTGAGATTTGT
	Reverse	CCCCAGAGACATGATGAAGTCA
Cathepsin K	Forward	CTTCCAATACGTGCAGCAGA
	Reverse	TCTTCAGGGCTTTCTCGTTC
NFATc1	Forward	CCGTTGCTTCCAGAAAATAACA
	Reverse	TGTGGGATGTGAACTCGGAA
DC-STAMP	Forward	AAAACCCTTGGGCTGTTCTT
	Reverse	AATCATGGACGACTCCTTGG
GAPDH	Forward	ACCCAGAAGACTGTGGATGG
	Reverse	CACATTGGGGGTAGGAACAC

and Akt signaling pathways, we treated cells with 5μM of AS for 4 hours, except the cells in the control group. Next, we added 50ng/mL of RANKL to cells for 5, 10, 20, 30, and 60 minutes. Additionally, we treated MC3T3-E1s with varying AS concentrations for 5 days for inducing osteogenic differentiation to determine the effect of AS on osteoblasts. Finally, we extracted total protein from cells in all groups using Radio-Immunoprecipitation Assay buffer + Phenylme-thylsulfonyl fluoride + phosphatase inhibitors (all Solarbio, Beijing, China). We separated protein samples on 10% SDS-PAGE, transferred them onto PVDF membranes (Millipore, CA, USA), and blocked them using QuickBlock™ Blocking Buffer (Beyotime) for 30 minutes at RT. Next, the proteins were incubated with primary antibodies at 4°C overnight and secondary antibodies at RT on rocking for 1 hour. We used chemiluminescent HRP Substrate (Millipore, CA, USA) and ImageQuant LAS 500 (GE Health Care, CT, USA) for detecting antibody reactivity. We quantitatively analyzed the intensity of bands with the aid of "Image J."

Mice Model of Ovariectomy (OVX)-induced Osteoporosis

To determine the effects of AS on bone destruction induced by osteoclasts, we used the OVX-induced osteoporosis mice model. All experiments involving animals were performed following the guidelines of the Animal Ethics Committee of Taizhou Hospital. The study was approved by the committee (ethical approval number: tzy-20233001). The 3Rs guidelines for animal welfare were followed for in vivo studies. We used healthy C57BL/6 female mice (8-week-olds, n=18) for in vivo studies. No significant difference in their physical condition was observed. First, mice were divided into the sham-operated, bilateral-OVX, and OVX injected with 20mg/kg AS groups (n=6/ group). Four weeks after surgery, in the sham-operated group, mice were administered PBS intraper-itoneally every 3 days. In the OVX group, mice were administered with PBS or 20mg/kg AS. After 4 weeks of treatment, all mice were euthanized, the femurs were harvested, and the soft tissues were cleaned. The tissues were fixed using 4% PFA and processed for subsequent analyses.

Micro-CT Scan

We analyzed the femur using high-resolution micro-CT (Scanco Medical, Wangen-Bruttisellen, Switzerland). For trabecular analysis, we selected the distal femur as the region of interest post-3D reconstruction. The status of bone trabeculae was determined by analyzing data selected for BV/TV, Tb.N, and Tb.Th.

Histopathologic Analysis

Following micro-CT scanning, we decalcified the femur by treating it with 10% EDTA for 21 days. Post complete decalcification, the femur was embedded in paraffin. The structure of the femur was visualized by staining with H&E and TRAP. The osteoclasts were stained with the TRAP kit, and the TRAP+ area was measured using the "Image J" software.

Statistical Analysis

All experiments were performed independently in triplicates to validate the results. We used the "GraphPad Prism" software (CA, USA) for statistically analyzing the results. The data were analyzed using a one-way analysis of variance, followed by the Tukey's test to compare the differences in the group. $P < 0.05$ indicated the significance level.

Results

AS-605240 Inhibits in vitro Differentiation of Osteoclast Induced by RANKL

First, we conducted the CCK-8 assay to determine AS toxicity on BMMs and identify safe AS concentrations. BMMs treated with < 5.0μM of AS were viable at 24, 48, 72, and 96 hours (Figure 1A). Therefore, 5.0μM was considered the maximum safe AS concentration for subsequent experiments.

Then, to determine the involvement of AS in the differentiation of osteoclasts, BMMs were stimulated with an osteoclast differentiation medium and AS of varying concentrations for 6 days. On day 6, a decrease in osteoclast differentiation was observed with decreasing AS concentration in the experimental group, and a significant increase in TRAP+ osteoclasts (nuclei > 3) was observed in the control group (Figure 1B and C). Finally, to analyze the effect of AS treatment at different osteoclast differentiation stages, BMMs were treated with AS at various stages of osteoclast differentiation, ie, on days 0–2, 2–4, 4–6, and 0–6. The results demonstrated that AS could significantly inhibit the formation of osteoclasts in the early and middle stages but had no effect on the final stages of osteoclastogenesis (Figure 1D and E).

Based on these results, we investigated if AS could inhibit osteoclast resorption in vitro. First, BMMs were seeded onto the bone fragments of bovine and treated with osteoclast differentiation media containing AS of varying concentrations. The results demonstrated a significant reduction in the resorption area of bone fragments treated with increasing AS concentration. Interestingly, a small resorption of bone fragments was observed on the treatment with 5.0μM of AS (Figure 2A and B).

Mature osteoclasts attach to the bone via the podosome belt on F-actin to mediate its effect.[24] Hence, phalloidin staining was performed on osteoclasts to determine the involvement of AS in podosome belt formation. Mature osteoclasts treated with AS formed smaller podosome belts compared to the control group (Figure 2C). A significant reduction in the area of podosome belts was observed in the treatment with 2.5 and 5.0μM of AS. These results show that AS could inhibit in vitro osteoclast differentiation-induced RANKL without cytotoxic effects.

AS-605240 Inhibits in vitro Osteoclast-Related Genes Triggered by RANKL

We used RT-qPCR to determine osteoclast-related gene expression. A decrease in Acp5, NFATc1, CTSK, and DC-STAMP (osteoclast-related genes) expression was observed at varying degrees on AS treatment (Figure 2D).

AS-605240 Inhibits Osteoclast Formation by Suppressing the PI3K/Akt Signaling Pathways

We determined the underlying mechanism of the effect of AS on osteoclasts. Several common signaling pathways are involved in the formation of osteoclasts. Therefore, we determined c-Fos and NFATc1 expression in BMMs stimulated with or without 5.0μM of AS and RANKL for 0, 1, 3, and 5 days. Next, we treated BMMs with 0, 1.25, 2.5, and 5.0μM of AS and RANKL for 5 days and measured NFATc1 and c-Fos protein expression. The results revealed an increase in c-Fos and NFATc1 expression levels from day 1 and a peak on day 3 in BMMs treated with RANKL; however, a decrease in c-Fos and NFATc1 expression levels was observed in AS-treated BMMs (Figure 3A and B). Moreover,
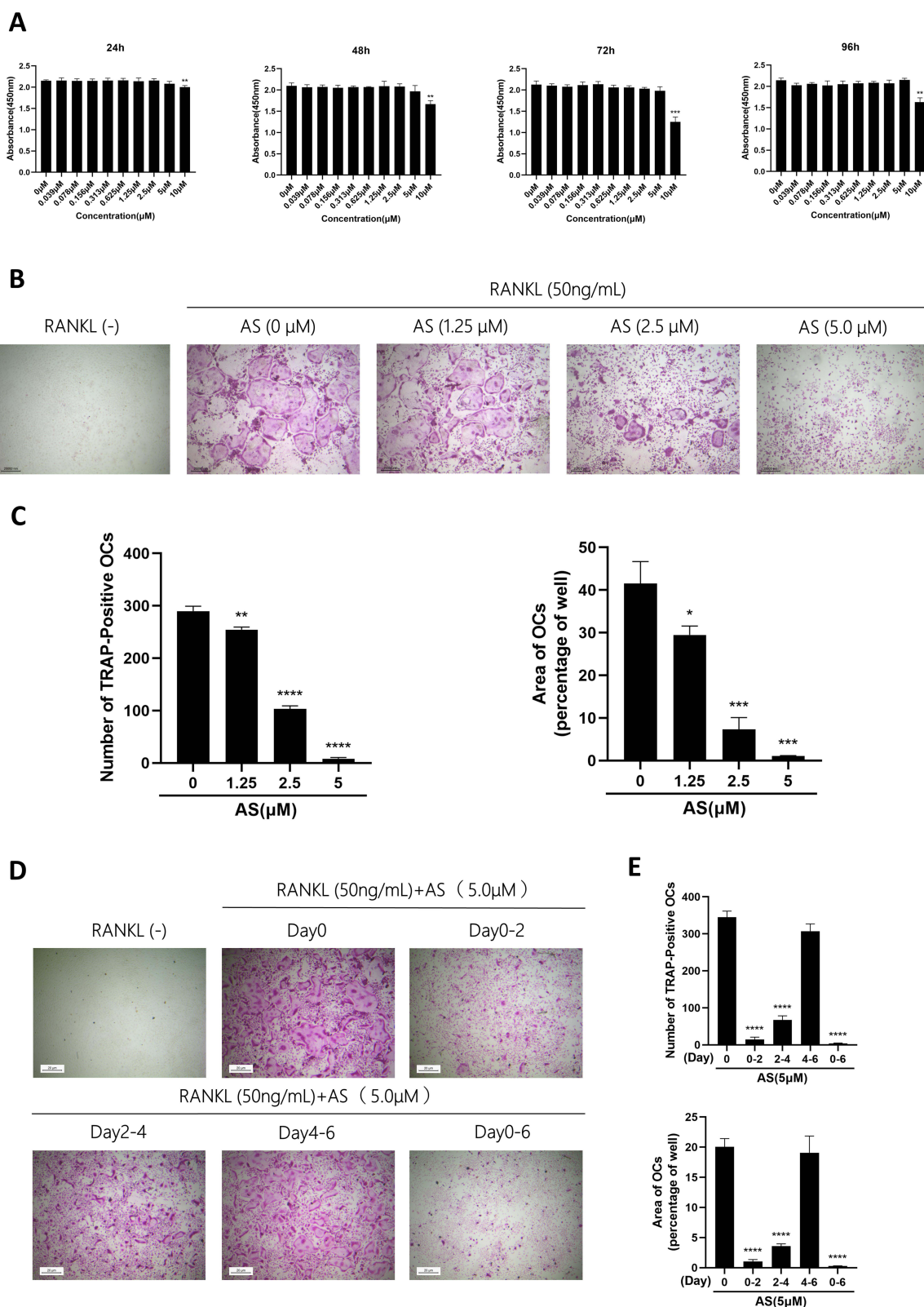
Figure 1 AS-605240 inhibits in vitro differentiation of osteoclast induced by RANKL. (**A**) The effect of AS on cell viability of BMMs by CCK-8 assay at 24, 48, 72, and 96h. (**B**) BMMs were treated with RANKL (50ng/mL) and M-CSF (30ng/mL) in the presence of 0, 1.25, 2.5, and 5.0μM AS for 6 days followed by TRAP staining. (**C**) Quantification of the number and area of TRAP+ cells with more than three nuclei. (**D**) Representative images of TRAP+ osteoclasts under treatment with 5.0μM AS at different times. (**E**) Quantification of the number and area of TRAP+ cells (nuclei > 3). *$p < 0.05$, **$p < 0.01$, ***$p < 0.001$, ****$P < 0.0001$. All data are expressed as mean ± SD.

A

B

C

D
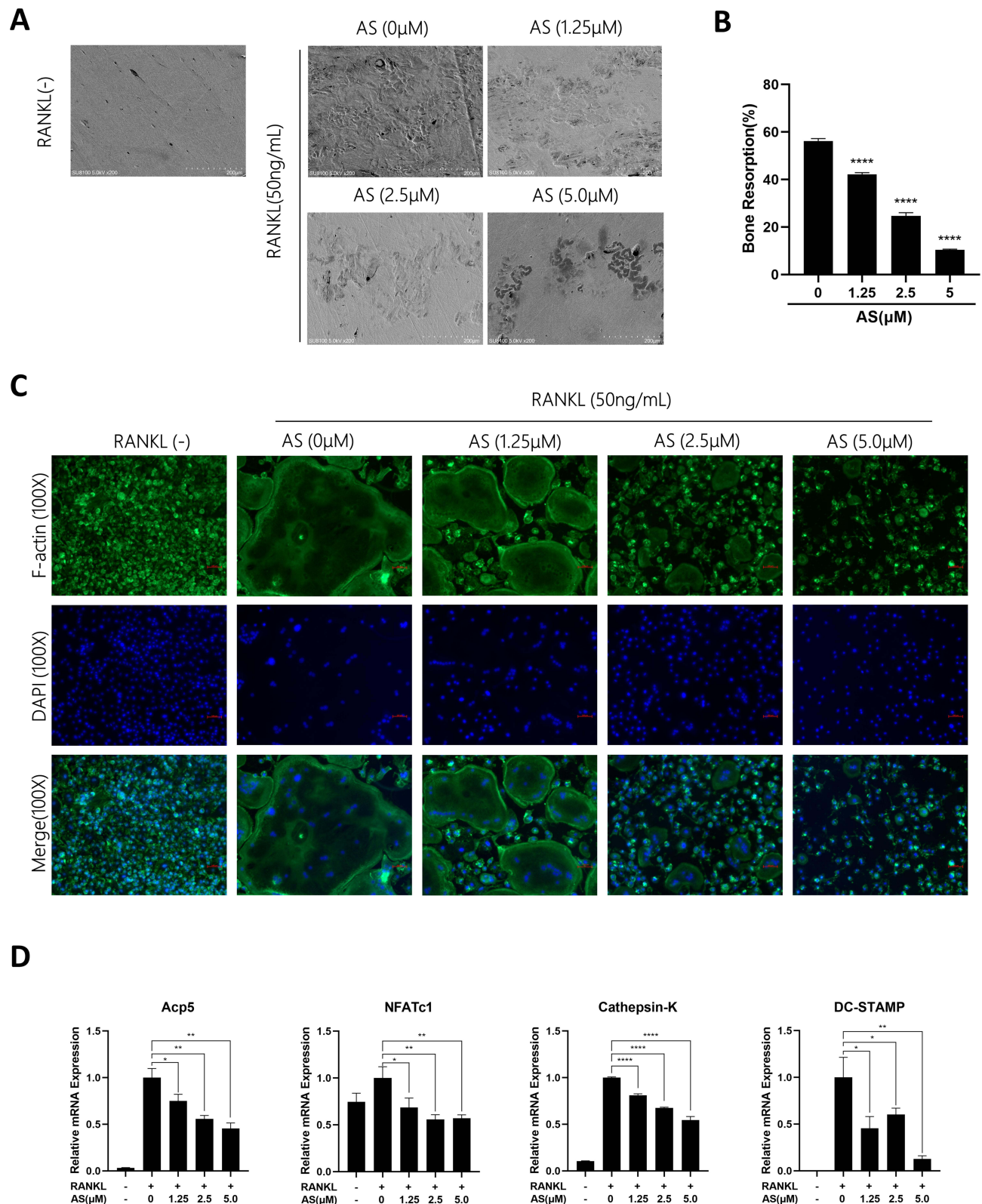
Figure 2 AS-605240 inhibits in vitro osteoclast-related genes triggered by RANKL. (**A**) BMMs were treated with RANKL (50ng/mL) and M-CSF (30ng/mL) in different concentrations of AS until mature osteoclasts formed and functioned. Scanning electron microscopy (SEM) showed images of bone resorption pits. (**B**) Quantification of bone resorption pit area with Image J (n = 3). (**C**) Observation of F-actin rings and nuclei in osteoclasts treated with different concentrations of AS by immunofluorescence microscopy. (**D**) The expression levels of osteoclast-associated genes were measured by RT-qPCR. The expression of these genes was normalized to the expression of GAPDH (n = 3). *p < 0.05, **p < 0.01, ****P < 0.0001. All data are expressed as mean ± SD.

a decrease in c-Fos and NFATc1 expression levels was observed following treating BMMs with increasing AS concentration (Figure 3C and D).

We treated BMMs with 0 or 5.0μM AS for 4 hours and 50ng/mL of RANKL for 0 to 60 minutes, to determine the alterations in the signaling pathways in the short term. A significant inhibition in PI3K and Akt phosphorylation was observed following treatment with AS over time (Figure 3E and F). However, no significant difference in the MAPK and NF-κB signaling pathway was observed in cells in the treatment and control groups (Figure 3G and H).

AS-605240 Enhances in vitro Osteoblast Activity

To test whether AS has an effect on osteoblast activity, we used the pre-osteoblast cell line MC3T3-E1s for the study. First, the effect of AS on the activity of the cell line was examined using a CCK-8 reagent. The results showed that MC3T3-E1s remained viable in culture for 96 hours when the AS concentration was lower than 1.25μM (Figure 4A). Next, MC3T3-E1s were cultured with osteogenic differentiation media containing varying AS concentrations for 7 days and stained using ALP reagent. Interestingly, an increase in MC3T3-E1s osteogenic activity was observed on treatment with 0.63μM of AS (Figure 4B). Furthermore, MC3T3-E1s were treated with the same concentration gradient for osteogenic differentiation. RT-qPCR and WB results demonstrated a significant increase in RUNX2 expression in MC3T3-E1s treated with 0.63μM of AS (Figure 4C-E). Together, these results indicate that 0.63μM of AS could significantly promote osteogenesis in vitro.

AS-605240 Inhibits OVX-Induced Osteoporosis in vivo

Finally, we determined if AS has therapeutic effects on OVX-induced osteoporosis in mice. We performed bilateral OVX in mice. Four weeks post-surgery, mice were administered 20mg/kg of AS or PBS every 3 days for 4 weeks. Next, the mice were euthanized, and the femur was harvested, fixed using 4% PFA, and analyzed by micro-CT scan. The scanned parameters showed a significant decrease in BV/TV, Tb.N, and Tb.Th in mice in the bilateral-OVX group injected with PBS compared to the sham-operated group. Furthermore, we observed an inhibition in bone loss in AS-treated mice in the bilateral-OVX group (Figure 5A and B).

After scanning, the femur was decalcified using 10% EDTA for 21 days and paraffin-embedded. Next, we performed H&E and TRAP staining on the femurs to analyze if AS could alleviate the bone loss. The staining results showed that AS alleviated bone loss due to OVX. Additionally, a significantly low mean TRAP+ cell area ratio was observed in mice in the bilateral OVX group injected with AS compared to the sham-operated group (Figure 5C and D). Thus, AS treatment could inhibit excess osteoclast formation.

Discussion

Osteoporosis is a bone metabolic disease that severely affects human health.[25,26] An imbalance in the remodeling of bone that favors either osteoclast or osteoblast activity significantly contributes to osteoporosis.[27] Several therapeutic agents available for mitigating disease progression have serious side effects when used for a longer duration.[28–30] Previous studies have demonstrated the significance of osteoclasts in osteoporosis, and inhibiting the PI3K signaling pathway could significantly reduce osteoclast production.[31,32] AS is a PI3Kγ inhibitor and has anti-inflammatory effects. Therefore, this study aimed to determine the anti-osteoclast effect of AS. Our results revealed that AS could inhibit osteoclasts in vitro, thereby indicating that AS could be used for treating patients with osteoporosis.

RANKL binds to RANK (cognate receptor) on the osteoclast surface to promote the differentiation of osteoclasts.[33] It also activates several important signaling pathways, thereby controlling the transformation of monocyte precursors to osteoclasts.[34] Our results demonstrated that AS attenuates the formation of osteoclasts in a concentration-dependent manner via the mechanism of inhibiting the PI3K/Akt-c-Fos/NFATc1 signaling axis mediated by RANKL. Furthermore, the MAPK and NF-κB signaling pathways also regulate the differentiation of osteoclasts induced by RANKL.[35–37] However, we did not observe the effect of AS on activating the MAPK and NF-κB signaling pathways.

The PI3K/Akt signaling pathway induces the differentiation of osteoclasts via NFATc1,[38] a transcription factor that regulates osteoclastogenesis-related gene expression.[39] A decrease in PI3K expression significantly affects osteoclastogenesis and reduces specific osteoclast-related gene and protein expression. We analyzed the expression profiles of
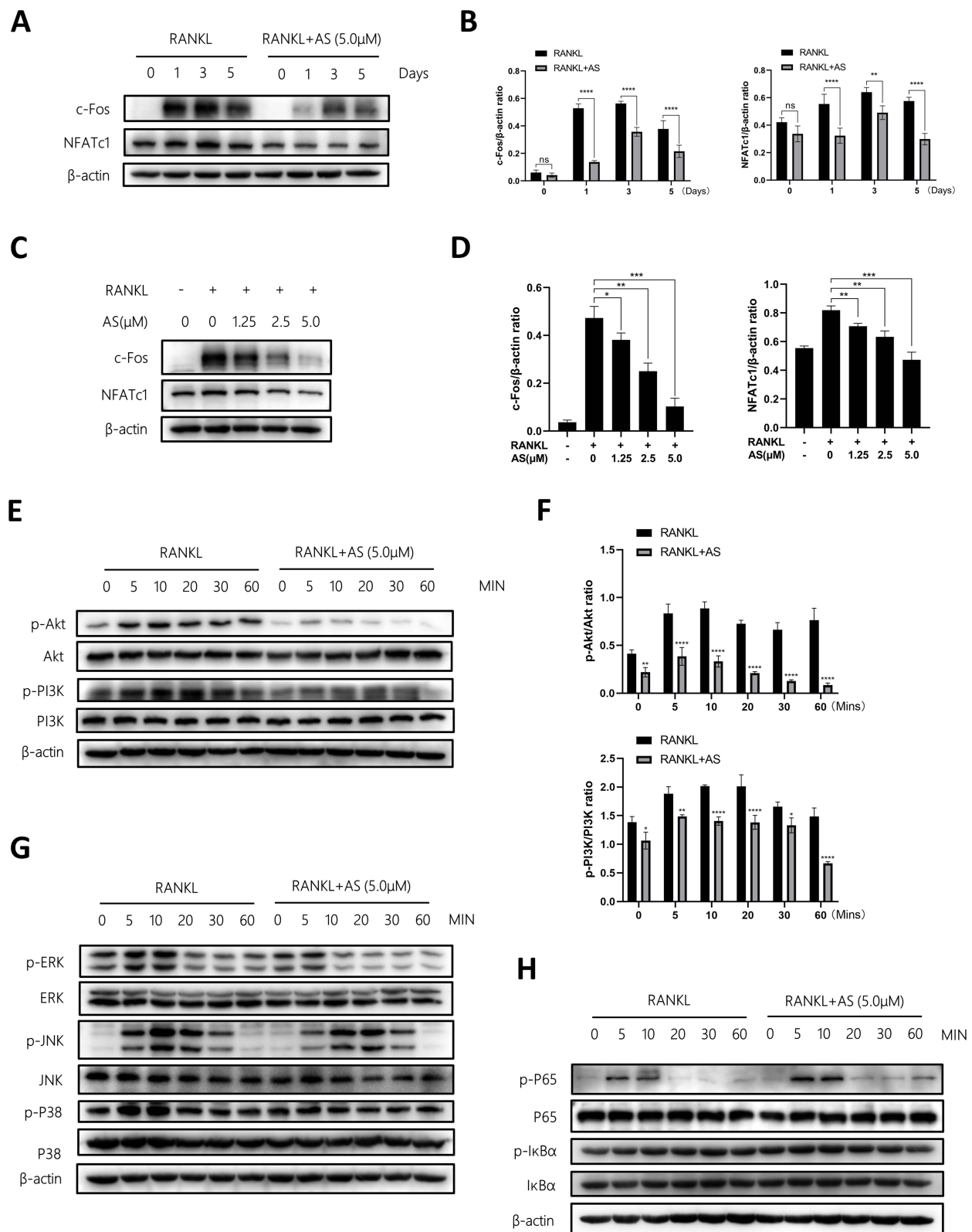
Figure 3 AS-605240 inhibits osteoclast formation by suppressing the PI3K/Akt signaling pathways. (**A**) BMMs were treated with or without AS (5μM) on days 1, 3, and 5, and the proteins of c-Fos and NFATc1 were detected by WB. (**B**) The expression levels of the above proteins were quantified to β-actin via ImageJ (n = 3). (**C**) The expression of c-Fos and NFATc1 in BMMs treated with different concentrations of AS was detected by WB. (**D**) The above proteins were quantified by image J to analyze the intensity of bands associated with β-actin (n = 3). (**E**) After BMMs were treated with AS (5μM), the expression of Akt signaling pathways was detected by WB at different time points. (**F**) Images of Akt pathway protein P-Akt/Akt and P-PI3K/PI3K expression were quantified using ImageJ (n = 3). (**G** and **H**) BMMs were pretreated with AS (5μM) and then stimulated with RANKL (50ng/mL) at different time points, and specific expression of MAPK and NF-κB signaling pathway was detected by WB. *p < 0.05, **p < 0.01, ***p < 0.001, ****P < 0.0001. All data are expressed as mean ± SD.
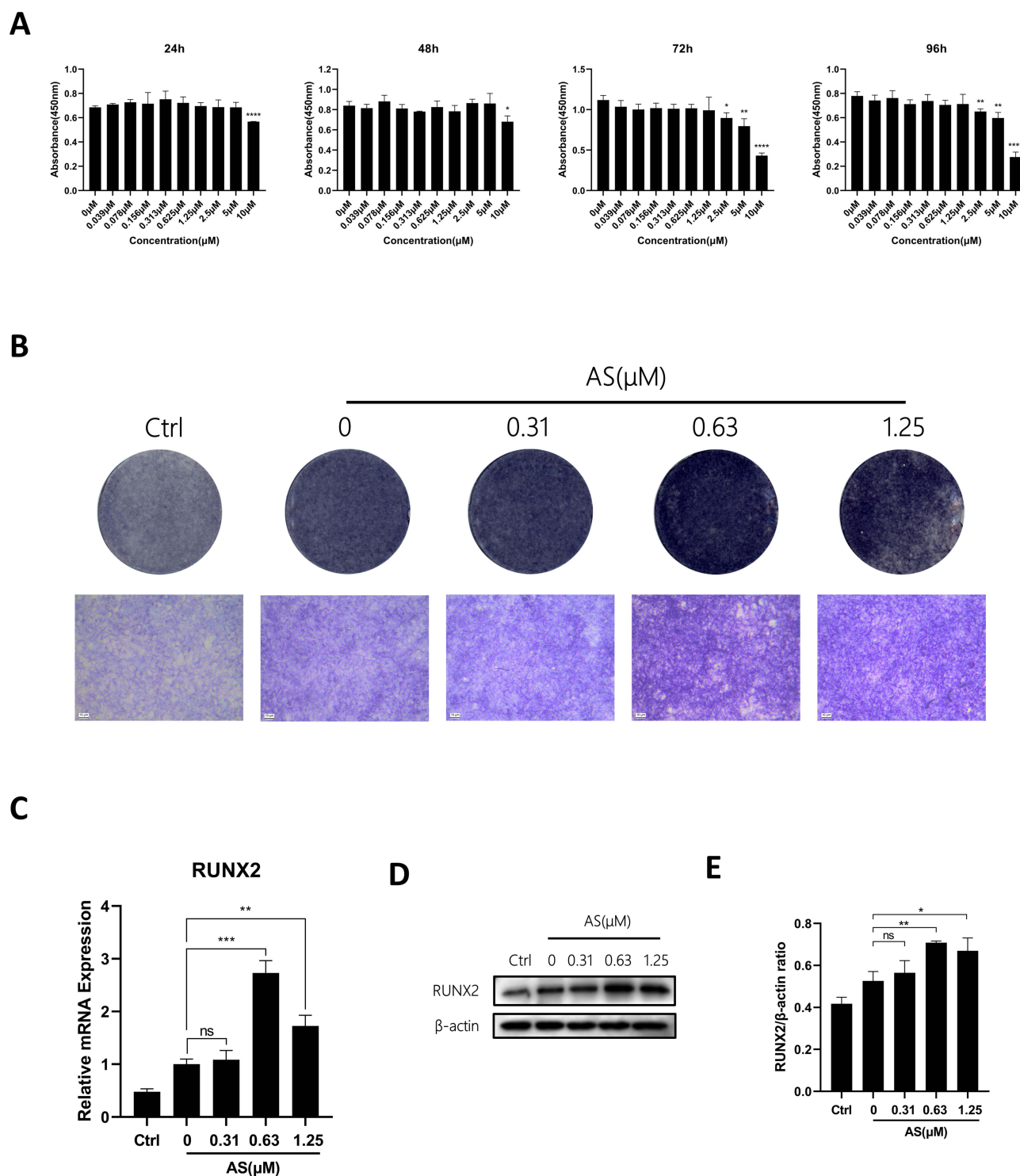
Figure 4 AS-605240 enhances in vitro osteoblast activity. (**A**) The effect of AS on cell viability of MC3T3-E1s by CCK-8 assay at 24, 48, 72, and 96h. (**B**) MC3T3-E1s were treated with osteogenic differentiation medium in the presence of 0, 0.31, 0.62, and 1.25μM AS for 7 days, followed by ALP staining. (**C**) The expression levels of osteoblast-associated genes were measured by RT-qPCR. The expression of these genes was normalized to the expression of GAPDH (n = 3). (**D**) The expression of RUNX2 in MC3T3-E1s treated with different concentrations of AS was detected by WB. (**E**) The above proteins were quantified by image J to analyze the intensity of bands associated with β-actin (n = 3). *p < 0.05, **p < 0.01, ***p < 0.001, ****P < 0.0001. All data are expressed as mean ± SD.
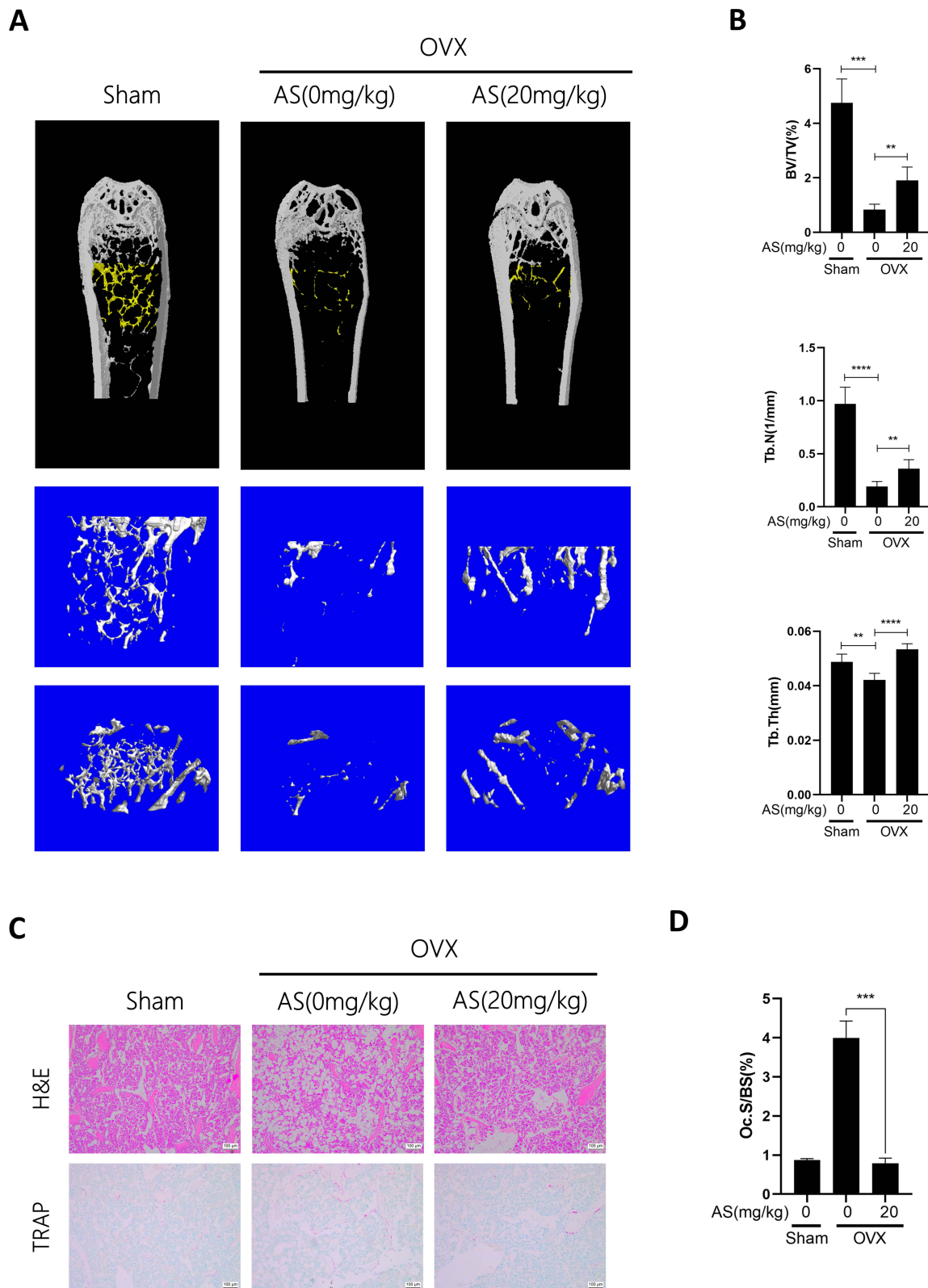
Figure 5 AS-605240 inhibits OVX-induced osteoporosis in vivo. (**A**) Representative micro-CT images of the distal femur were taken from the collected femur of different groups of mice. (**B**) Quantitative analysis of BV/TV, Tb.N, and Tb.Th was performed with micro-CT sky scan software. (**C**) Representative graphs of H&E and TRAP staining of femoral sections from different groups of mice. (**D**) Quantitative analysis was performed on Oc.S/BS. **p < 0.01, ***p < 0.001, ****P < 0.0001. All data are expressed as mean ± SD.

osteoclastogenesis-related genes to determine if AS attenuated osteoclastogenesis by inhibiting NFATc1. The result revealed a decrease in Acp5, CTSK, and DC-STAMP expression levels.

Bone remodeling is a complex and rigorous process that relies on the close interaction between osteoclasts and osteoblasts to maintain homeostasis. Moreover, osteoblasts are significantly involved in the bone remodeling process. It synthesizes the bone matrix, controls mineralization, and differentiates into osteocytes or bone lining cells.[27] To analyze the effect of AS on the formation of osteoblasts, we treated MC3T3-E1s with AS in a dose-dependent manner. Unlike other drugs inhibiting osteoclast activity, AS could attenuate osteoclast differentiation and promote the osteoblast-forming ability of MC3T3-E1s.

Next, we analyzed the therapeutic effect of AS in OVX-induced osteoporosis in mice. Our results showed that mice in the bilateral-OVX group injected with PBS showed more bone loss compared to mice injected with AS. Our in vitro results were verified using animal experiments. A decrease in TRAP+ osteoclasts was observed in the femur of AS-treated mice. This result suggests that the inhibition of osteoclasts by AS is involved in bone loss in mice.

However, our study has a few limitations. For the maintenance of bone homeostasis, bone destruction and bone formation activity of osteoblasts should be regulated. In vitro results showed that AS inhibits osteoclast bone resorption and enhances osteoblast activity. However, additional studies are required to determine the mechanism of action of AS on osteoblasts and osteoclasts under co-culture conditions.

Conclusion

In summary, we demonstrated that AS inhibits the PI3K/Akt-c-Fos/NFATc1 signaling pathway to suppress osteoclast activity, thus preventing bone loss caused by OVX. Next, AS promotes osteoblast differentiation. These results show the functions of AS and provide a new approach to treating osteolytic osteoporosis.

Abbreviations

BMMs, bone marrow macrophages; M-CSF, macrophage colony-stimulating factor; RANKL, receptor activator nuclear factor-kappa B ligand; PI3K/Akt, phosphatidylinositol 3-kinase/protein kinase B; MAPK, Mitogen-activated protein kinase; NF-κB, nuclear factor-κB; BV/TV, Bone surface /volume ratio; Tb.N, Number of bone trabeculae; Tb.Th, Bone trabeculae thickness.

Ethics Approval and Informed Consent

All experiments involving animals were performed following the guidelines of the Animal Ethics Committee of Taizhou Hospital. The study was approved by the committee (ethical approval number: tzy-20233001). The 3Rs guidelines for animal welfare were followed for in vivo studies.

Acknowledgments

We thank the public experimental platform of Taizhou Hospital affiliated to Wenzhou Medical University for providing the research environment and experimental technical support.

Author Contributions

All authors contributed to data analysis, drafting or revising the article, have agreed on the journal to which the article will be submitted, gave final approval of the version to be published, and agree to be accountable for all aspects of the work.

Funding

Disclosure

No author has an actual or perceived conflict of interest with the contents of this article.

References

1. Li X, Wang L, Huang B, et al. Targeting actin-bundling protein L-plastin as an anabolic therapy for bone loss. *Sci Adv*. 2020;6(47). doi:10.1126/sciadv.abb7135
2. Christenson RH. Biochemical markers of bone metabolism: an overview. *Clin Biochem*. 1997;30(8):573–593. doi:10.1016/S0009-9120(97)00113-6
3. Li L, Sapkota M, Kim SW, Soh Y. Herbacetin inhibits RANKL-mediated osteoclastogenesis in vitro and prevents inflammatory bone loss in vivo. *Eur J Pharmacol*. 2016;777:17–25. doi:10.1016/j.ejphar.2016.02.057
4. Zhao C, Irie N, Takada Y, et al. Bidirectional ephrinB2-EphB4 signaling controls bone homeostasis. *Cell Metab*. 2006;4(2):111–121. doi:10.1016/j.cmet.2006.05.012
5. Huang JM, Ren RY, Bao Y, et al. Ulinastatin Inhibits Osteoclastogenesis and Suppresses Ovariectomy-Induced Bone Loss by Downregulating uPAR. *Front Pharmacol*. 2018;9:1016. doi:10.3389/fphar.2018.01016
6. Li Q, Wang M, Xue H, et al. Ubiquitin-Specific Protease 34 Inhibits Osteoclast Differentiation by Regulating NF-κB Signaling. *J Bone Miner Res*. 2020;35(8):1597–1608. doi:10.1002/jbmr.4015
7. Theill LE, Boyle WJ, Penninger JM. RANK-L and RANK: t cells, bone loss, and mammalian evolution. *Annu Rev Immunol*. 2002;20:795–823. doi:10.1146/annurev.immunol.20.100301.064753
8. Teitelbaum SL. Bone resorption by osteoclasts. *Science*. 2000;289(5484):1504–1508. doi:10.1126/science.289.5484.1504
9. Ono T, Nakashima T. Recent advances in osteoclast biology. *Histochem Cell Biol*. 2018;149(4):325–341. doi:10.1007/s00418-018-1636-2
10. Lampiasi N, Russo R, Zito F. The Alternative Faces of Macrophage Generate Osteoclasts. *Biomed Res Int*. 2016;2016:9089610. doi:10.1155/2016/9089610
11. Boyle WJ, Simonet WS, Lacey DL. Osteoclast differentiation and activation. *Nature*. 2003;423(6937):337–342. doi:10.1038/nature01658
12. Kawamura N, Kugimiya F, Oshima Y, et al. Akt1 in osteoblasts and osteoclasts controls bone remodeling. *PLoS One*. 2007;2(10):e1058. doi:10.1371/journal.pone.0001058
13. Quan GH, Wang H, Cao J, et al. Calycosin Suppresses RANKL-Mediated Osteoclastogenesis through Inhibition of MAPKs and NF-κB. *Int J Mol Sci*. 2015;16(12):29496–29507. doi:10.3390/ijms161226179
14. Negishi-Koga T, Takayanagi H. Ca2+-NFATc1 signaling is an essential axis of osteoclast differentiation. *Immunol Rev*. 2009;231(1):241–256. doi:10.1111/j.1600-065X.2009.00821.x
15. Kim K, Kim JH, Lee J, et al. Nuclear factor of activated T cells c1 induces osteoclast-associated receptor gene expression during tumor necrosis factor-related activation-induced cytokine-mediated osteoclastogenesis. *J Biol Chem*. 2005;280(42):35209–35216. doi:10.1074/jbc.M505815200
16. Peng J, Zhao K, Zhu J, et al. Sarsasapogenin Suppresses RANKL-Induced Osteoclastogenesis in vitro and Prevents Lipopolysaccharide-Induced Bone Loss in vivo. *Drug Des Devel Ther*. 2020;14:3435–3447. doi:10.2147/DDDT.S256867
17. Azzi J, Moore RF, Elyaman W, et al. The novel therapeutic effect of phosphoinositide 3-kinase-gamma inhibitor AS605240 in autoimmune diabetes. *Diabetes*. 2012;61(6):1509–1518. doi:10.2337/db11-0134
18. Camps M, Ruckle T, Ji H, et al. Blockade of PI3Kgamma suppresses joint inflammation and damage in mouse models of rheumatoid arthritis. *Nat Med*. 2005;11(9):936–943. doi:10.1038/nm1284
19. Barber DF, Bartolome A, Hernandez C, et al. PI3Kgamma inhibition blocks glomerulonephritis and extends lifespan in a mouse model of systemic lupus. *Nat Med*. 2005;11(9):933–935. doi:10.1038/nm1291
20. Horiguchi M, Oiso Y, Sakai H, Motomura T, Yamashita C. Pulmonary administration of phosphoinositide 3-kinase inhibitor is a curative treatment for chronic obstructive pulmonary disease by alveolar regeneration. *J Control Release*. 2015;213:112–119. doi:10.1016/j.jconrel.2015.07.004
21. Li M, Sala V, De Santis MC, et al. Phosphoinositide 3-Kinase Gamma Inhibition Protects From Anthracycline Cardiotoxicity and Reduces Tumor Growth. *Circulation*. 2018;138(7):696–711. doi:10.1161/CIRCULATIONAHA.117.030352
22. Wei L, Chen W, Huang L, et al. Alpinetin ameliorates bone loss in LPS-induced inflammation osteolysis via ROS mediated P38/PI3K signaling pathway. *Pharmacol Res*. 2022;184:106400. doi:10.1016/j.phrs.2022.106400
23. Yang S, Song D, Wang Z, et al. AKT/GSK3β/NFATc1 and ROS signal axes are involved in AZD1390-mediated inhibitory effects on osteoclast and OVX-induced osteoporosis. *Int Immunopharmacol*. 2022;113(Pt A):109370. doi:10.1016/j.intimp.2022.109370
24. Xian Y, Su Y, Liang J, et al. Oroxylin A reduces osteoclast formation and bone resorption via suppressing RANKL-induced ROS and NFATc1 activation. *Biochem Pharmacol*. 2021;193:114761. doi:10.1016/j.bcp.2021.114761
25. Tai TW, Chen CY, Su FC, et al. Reactive oxygen species are required for zoledronic acid-induced apoptosis in osteoclast precursors and mature osteoclast-like cells. *Sci Rep*. 2017;7:44245. doi:10.1038/srep44245
26. Hu Y, Li X, Zhi X, et al. RANKL from bone marrow adipose lineage cells promotes osteoclast formation and bone loss. *EMBO Rep*. 2021;22(7):e52481. doi:10.15252/embr.202152481
27. Kular J, Tickner J, Chim SM, Xu J. An overview of the regulation of bone remodelling at the cellular level. *Clin Biochem*. 2012;45(12):863–873. doi:10.1016/j.clinbiochem.2012.03.021
28. Paschalis EP, Gamsjaeger S, Hassler N, et al. Vitamin D and calcium supplementation for three years in postmenopausal osteoporosis significantly alters bone mineral and organic matrix quality. *Bone*. 2017;95:41–46. doi:10.1016/j.bone.2016.11.002
29. AlRahabi MK, Ghabbani HM. Clinical impact of bisphosphonates in root canal therapy. *Saudi Med J*. 2018;39(3):232–238. doi:10.15537/smj.2018.3.20923
30. Cui J, Li X, Wang S, et al. Triptolide prevents bone loss via suppressing osteoclastogenesis through inhibiting PI3K-AKT-NFATc1 pathway. *J Cell Mol Med*. 2020;24(11):6149–6161. doi:10.1111/jcmm.15229
31. Da W, Tao L, Zhu Y. The role of osteoclast energy metabolism in the occurrence and development of osteoporosis. *Front Endocrinol (Lausanne)*. 2021;12:675385. doi:10.3389/fendo.2021.675385
32. Fu L, Wu W, Sun X, Zhang P. Glucocorticoids Enhanced Osteoclast Autophagy Through the PI3K/Akt/mTOR Signaling Pathway. *Calcif Tissue Int*. 2020;107(1):60–71. doi:10.1007/s00223-020-00687-2

33. Li J, Sarosi I, Yan XQ, et al. RANK is the intrinsic hematopoietic cell surface receptor that controls osteoclastogenesis and regulation of bone mass and calcium metabolism. *Proc Natl Acad Sci U S A*. 2000;97(4):1566–1571. doi:10.1073/pnas.97.4.1566

34. Boyce BF. Advances in the regulation of osteoclasts and osteoclast functions. *J Dent Res*. 2013;92(10):860–867. doi:10.1177/0022034513500306

35. Rahman MM, Kukita A, Kukita T, Shobuike T, Nakamura T, Kohashi O. Two histone deacetylase inhibitors, trichostatin A and sodium butyrate, suppress differentiation into osteoclasts but not into macrophages. *Blood*. 2003;101(9):3451–3459. doi:10.1182/blood-2002-08-2622

36. Yamanaka Y, Clohisy JC, Ito H, Matsuno T, Abu-Amer Y. Blockade of JNK and NFAT pathways attenuates orthopedic particle-stimulated osteoclastogenesis of human osteoclast precursors and murine calvarial osteolysis. *J Orthop Res*. 2013;31(1):67–72. doi:10.1002/jor.22200

37. Lee SE, Woo KM, Kim SY, et al. The phosphatidylinositol 3-kinase, p38, and extracellular signal-regulated kinase pathways are involved in osteoclast differentiation. *Bone*. 2002;30(1):71–77. doi:10.1016/S8756-3282(01)00657-3

38. Liou SF, Hsu JH, Lin IL, et al. KMUP-1 suppresses RANKL-induced osteoclastogenesis and prevents ovariectomy-induced bone loss: roles of MAPKs, Akt, NF-κB and calcium/calcineurin/NFATc1 pathways. *PLoS One*. 2013;8(7):e69468. doi:10.1371/journal.pone.0069468

39. Takayanagi H. The role of NFAT in osteoclast formation. *Ann N Y Acad Sci*. 2007;1116:227–237. doi:10.1196/annals.1402.071